Physics of the Earth and Planetary Interiors 182 (2010) 59–72

Contents lists available at ScienceDirect

Physics of the Earth and Planetary Interiors

journal homepage: www.elsevier.com/locate/pepi

Frequency-dependent shear wave splitting and heterogeneous anisotropic structure beneath the Gulf of California region

Maureen D. Long*

Department of Geology and Geophysics, Yale University, PO Box 208109, New Haven, CT 06520, United States

ARTICLE INFO

Article history:
Received 30 May 2009
Received in revised form 24 March 2010
Accepted 22 June 2010

Edited by: Prof. G. Helffrich.

Keywords:
Shear wave splitting
Seismic anisotropy
Upper mantle
Gulf of California
SKS
Frequency dependence

ABSTRACT

The Gulf of California region has undergone a major evolution over the past ~15 Ma, since subduction of the now-extinct Farallon plate ceased and transform motion began, leading to the initiation of rifting and the opening of the Gulf of California ~5 Ma ago. The character of dynamic processes in the upper mantle beneath the region remains poorly understood, but constraints on seismic anisotropy in the upper mantle can shed light on contemporary mantle flow processes. In order to characterize more fully the anisotropic structure of the upper mantle beneath the region, I present measurements of SKS splitting at 14 broadband stations of the NARS-Baja array at periods between ~8 and 50 s. The measured splitting parameters (ϕ, δt) at NARS-Baja stations exhibit a high degree of complexity, with dramatic lateral variations, significant backazimuthal variations at individual stations, and a large number of well-constrained null measurements over a range of backazimuths. The dependence of splitting parameters on frequency is evaluated by applying a series of bandpass filters to high signal-to-noise SKS arrivals. I find that while fast directions are generally insensitive to the SKS frequency content, delay times are frequency dependent at several stations. The measurements presented in this study indicate that the anisotropic structure of the upper mantle beneath the Gulf of California region is complex and exhibits a high degree of both lateral and vertical heterogeneity. The observed splitting is consistent with a scenario in which a large-scale reorganization of the mantle flow field has been inhibited by the presence of a stalled fragment of oceanic lithosphere associated with Farallon subduction. The pattern of mantle flow appears to be controlled by more localized processes, likely including small-scale buoyant upwelling associated with partial melting beneath the central part of the Gulf of California rift.

1. Introduction

The region surrounding the Gulf of California has a complex recent tectonic history that includes the cessation of Farallon plate subduction at ~15 Ma and the subsequent transfer of Baja California to the Pacific plate and initiation of rifting in the Gulf (e.g., Atwater, 1970; Stock and Hodges, 1989; Michaud et al., 2006). The region has therefore undergone a fairly rapid evolution from a continental arc setting to a transform boundary that accommodates both strike-slip motion and extension associated with oblique rifting. The geometry of upper mantle flow has likely also undergone a rapid evolution over recent geological history, from the flow field associated with Farallon subduction to that associated with the present-day tectonic setting. Many fundamental questions about such a temporal evolution of mantle flow remain unanswered; for example, little is known about the timescale over which a complete reorganization of the local upper mantle flow field can be accomplished. In order to begin to understand how the pattern of upper mantle flow beneath the Gulf of California has evolved through time, a detailed characterization of the present-day flow patterns is necessary.

Measurements of upper mantle seismic anisotropy yield some of the most direct constraints we have on the geometry of (present-day) mantle flow, so investigations of anisotropic structure can help to elucidate the links between dynamic mantle processes at depth and surface tectonics. Seismic anisotropy in the upper mantle is generally understood to result from the lattice-preferred orientation (LPO) of mantle minerals (primarily olivine) and if the relationship between finite strain and the resulting anisotropy is properly characterized, then the pattern of mantle flow can be inferred from anisotropic geometry (e.g., Karato et al., 2008). In practice, however, it can be difficult to discriminate between "frozen-in" lithospheric mantle anisotropy, which reflects past deformational processes, and anisotropy in the asthenosphere, which is indicative of present-day mantle flow. Additionally, there may be ambiguity about the geometrical relationship between strain and anisotropy, which will depend on the olivine fabric type (which, in turn, depends on the physical conditions of deformation,

* Tel.: +1 203 432 5031.
E-mail address: maureen.long@yale.edu.

0031-9201/$ – see front matter © 2010 Elsevier B.V. All rights reserved.
doi:10.1016/j.pepi.2010.06.005

such as the temperature, differential stress, pressure, and volatile content; Karato et al., 2008). Because LPO develops over a finite timescale, the anisotropy of a volume of mantle rock will depend on its deformation history and in flow fields that vary rapidly over short length scales, LPO development may "lag" mantle flow (e.g., Kaminski and Ribe, 2002). Finally, the shape-preferred orientation (SPO) of partial melt may play a role in controlling anisotropy in volcanic regions (e.g., Vauchez et al., 2000; Holtzman et al., 2003) at the depth range relevant for melt production (thought to be ~40–90 km beneath the Gulf of California; Wang et al., 2009). In the presence of significant partial melt, the usual relationships between flow and anisotropy (via LPO) may not hold.

Anisotropic structure manifests itself in the seismic wavefield in several ways, but the splitting or birefringence of shear waves is a direct indicator of anisotropy and splitting measurements on SKS phases provide constraints on anisotropy directly beneath a seismic station (for a recent review, see Long and Silver, 2009). SKS phases have nearly vertical paths through the upper mantle, which in practice means that the depth resolution is poor but the lateral resolution is excellent. The lack of depth resolution can be addressed, at least in part, by combining SKS splitting with other observational constraints that better constrain the depth extent of anisotropy, such as surface wave or receiver function analysis or the splitting of local earthquakes. Despite the difficulties with interpretation, however, shear wave splitting represents one of the most powerful tools available to characterize mantle flow in active tectonic regions. SK*S splitting in the Gulf of California region has previously been investigated by Obrebski et al. (2006) and van Benthem et al. (2008), who examined broadband data for the northern and southern parts of the region, respectively. Each of these studies examined approximately 2–3 years' worth of data from NARS-Baja stations; these authors generally identified a few (3–10) well-constrained measurements per station.

In the study presented here, I expand upon the previous work by Obrebski et al. (2006) and van Benthem et al. (2008) and present measurements of SKS splitting at the 14 stations of the NARS-Baja network (Trampert et al., 2003) for the period between early 2002 and mid-2007. A specific aim of this study is to understand whether the SKS splitting beneath individual stations in the Gulf of California region is consistent with a single, horizontal, homogenous layer of anisotropy or a more complex anisotropic structure. I examined SKS splitting for events over a wide range of backazimuths and sought to identify any stations that exhibit a clear backazimuthal dependence on splitting parameters. I also investigated the dependence of SKS splitting parameters on frequency, which is likely an indication of lateral and/or vertical heterogeneity in anisotropic structure (e.g., Long and Silver, 2009). I focused initially on measuring splitting for SKS energy at periods greater than 8–10 s using multiple measurement methods; this produced a splitting dataset complementary to that of Obrebski et al. (2006) and van Benthem et al. (2008), who examined SKS splitting at periods between 1 and 25 s using the method of Silver and Chan (1991). There are significant discrepancies between previous measurements that included higher-frequency energy and those presented in this paper; such disparities are an indication of frequency-dependent splitting. In order to investigate this dependence further, the highest-quality waveforms in the dataset were identified and subjected to a series of bandpass filters and the dependence of splitting parameters on frequency was investigated in detail. The possibility of a contribution from lower mantle anisotropy to the SKS splitting dataset was also considered, as SKS–SKKS splitting discrepancies have been previously identified at NARS-Baja stations and attributed to azimuthal anisotropy in the lowermost mantle (Long, 2009). The specific goal of this study is to use frequency-dependent SKS splitting to elucidate the present-day pattern of mantle flow beneath the Gulf of California, to understand what processes control this pattern, and to understand mantle flow in the context of the recent tectonic history of the region.

2. Tectonic, geological, and geophysical setting

The continental margin in the vicinity of the present-day Gulf of California has undergone a dramatic tectonic evolution over the past ~15 Ma. Long-lived subduction of the Farallon plate beneath North America ceased as the Mendocino triple junction migrated northward (e.g., Atwater, 1970; Bohannon and Parsons, 1995) and the remnant of the Farallon plate broke into the Magdelena and Guadalupe microplates, which are thought to remain lodged beneath Baja California (e.g., Michaud et al., 2006, and references therein). The margin thus underwent a transition from a convergent arc setting to a transform boundary; the extensional component of the Pacific–North America plate motion resulted in incipient oblique rifting in the former backarc (what is now the Gulf of California) and the transfer of Baja California to the Pacific Plate (e.g., Stock and Hodges, 1989). Oskin et al. (2001) argue that this plate transfer post-dated the cessation of subduction by ~6 Ma and that the localization of Pacific–North America plate motion in the Gulf of California at ~5 Ma ago was geologically rapid.

The present-day relative motion between the Pacific and North American plates is largely accommodated (~90%) by oblique rifting in the Gulf of California (Dixon et al., 2000) along short rift segments that are connected by longer transform faults (e.g., Sedlock, 2003; Lizzaralde et al., 2007). To the south, the Gulf of California rift system transitions into the East Pacific Rise spreading system; to the north, it transitions into the strike-slip San Andreas fault system. Geologically and structurally, Baja California makes up the Baja Peninsular Range, composed of subduction-related arc volcanics; this region is not undergoing significant present-day extension and moves as a rigid block. To the east of the Gulf of California is the southernmost part of the Basin and Range province, which has undergone significant extension beginning in the early Miocene (e.g., Henry, 1989; Suter and Contreras, 2002).

In addition to the constraints on the tectonic history of the region derived from geological studies and plate reconstructions, there are constraints on the structure of the crust and mantle at depth derived from geophysical studies, which are particularly useful for contextualizing the interpretation of shear wave splitting measurements. The upper mantle velocity structure beneath the Gulf of California and adjacent regions has been studied by Zhang et al. (2007, 2009) using Rayleigh wave dispersion measurements; they found that upper mantle velocities in this region are considerably lower than global averages, consistent with the results of global surface wave inversions (e.g., Lebedev and van der Hilst, 2008; Nettles and Dziewonski, 2008). These low velocities are consistent with high upper mantle temperatures and/or the presence of melt and indicate that the lithosphere beneath the region is likely thin. Zhang et al. (2009) identified a relatively high-velocity anomaly in the central Gulf at depths between 120 and 150 km, which they interpret to be a lodged fragment of the Guadalupe slab. These workers also mapped the 2ψ azimuthal anisotropy as a function of period and their measurements indicate that the anisotropic structure of the upper mantle beneath the region is complex, with both lateral and vertical heterogeneity.

Obrebski and Castro (2008) also argued for the presence of a wedge fragment(s) of the remnant Farallon slab beneath Baja California from anisotropic receiver function analysis; this study also characterized crustal anisotropy beneath three NARS-Baja stations (NE71, NE75, and NE81). Receiver function analysis has also been used to map the depth of the Moho in the northern part of the Gulf of California (Lewis et al., 2001) and for stations of the NARS-Baja array (Persaud et al., 2007). Crustal thicknesses vary considerably along

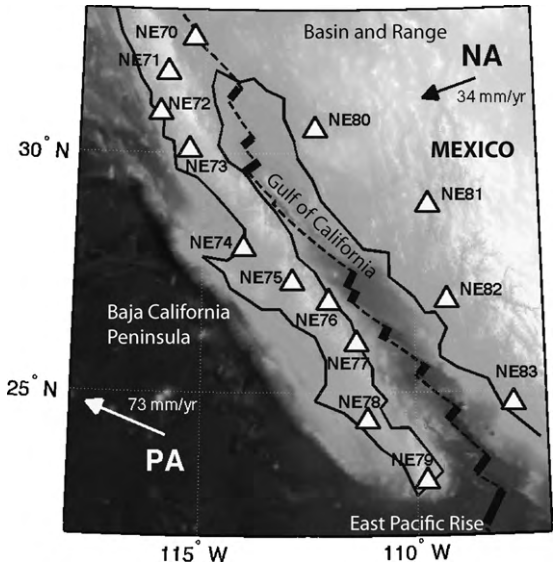

Fig. 1. Map of the NARS-Baja broadband network (triangles). The Gulf of California plate boundary from the University of Texas digital database (Coffin et al., 1998) is shown with a dashed line; the short active rift segments are shown with thick black lines. The arrows indicate the absolute plate motion (APM) of the North American (NA) and Pacific (PA) plates in the HS3-Nuvel1A reference frame (Gripp and Gordon, 2002).

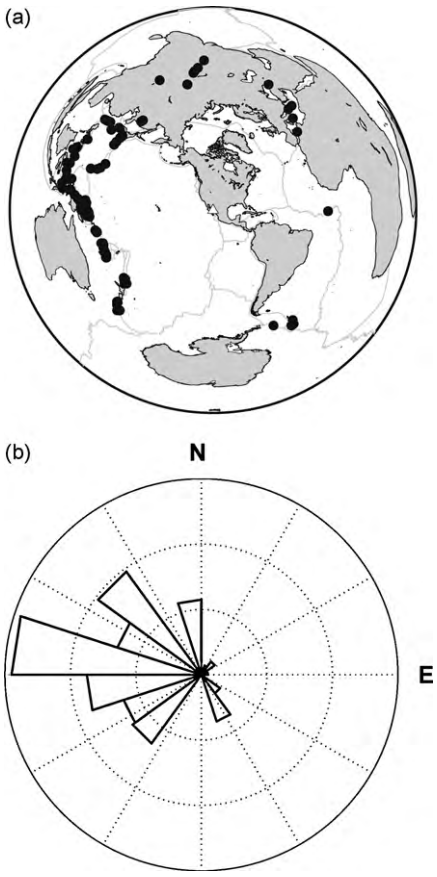

Fig. 2. (a) A map of earthquakes (black dots) that yielded at least one well-constrained SKS splitting measurement (null or non-null). The approximate center of the NARS-Baja array is shown with a triangle. (b) Circular histogram of back-azimuthal coverage in the full dataset (again including both null and non-null measurements).

strike; to the east of the Gulf, the Moho is generally shallower than ~30 km, while along the Peninsular Range crustal thickness values vary from ~20 to ~35 km and appear to be uncorrelated with topography (Persaud et al., 2007). The crustal structure of three segments of the rift itself was investigated by Lizzaralde et al. (2007) using wide-angle seismic data and they found evidence for significant along-strike variations in the style of rifting, crustal thickness in the vicinity of the rift center, degree of mantle melting, and degree of sedimentation. They concluded that these along-strike variations were likely due to differences in inherited mantle fertility and point to the effect of inherited pre-rift tectonic structures produced by convergent margin processes.

3. Data and methods

I utilized data from the 14 broadband stations of the Network of Autonomously Recording Seismographs (NARS)-Baja array, operated jointly by the Universiteit Utrecht, the California Institute of Technology, and the Centro de Investigación Científica y de Educación Superior de Ensenada (CICESE) (Trampert et al., 2003). The array, which was composed of STS-2 seismometers, was installed in early to mid-2002 and most stations ran through mid- to late 2007. Data from the period 3/2002–3/2007 were examined in this study; the station locations are shown in Fig. 1. Events with magnitudes $\geq$5.8 at epicentral distances from 88° to 120° were selected for analysis (Fig. 2). The preprocessing and splitting measurements were carried out using the SplitLab software package (Wüstefeld et al., 2007). A bandpass filter with corner frequencies at 0.01 and 0.1 Hz was applied to all data and a time window around the expected SKS arrival time from the iasp91 travel time tables was visually inspected for each event–station pair to identify SKS arrivals with high signal-to-noise ratio (SNR) and good waveform clarity. In some cases, the corner frequencies on the bandpass filter were adjusted to optimize the signal quality, but in all cases energy at periods between 8–10 and 25–50 s was retained. The windows for the splitting analyses were chosen manually and covered at least one full period of the SKS signal.

Several steps were taken to ensure the highest possible measurement quality in the dataset. First, two different measurement methods were used; both the transverse component minimization method of Silver and Chan (1991) and the rotation-correlation (also known as cross-correlation) method were applied to the data simultaneously. Several studies have demonstrated that these measurement methods can disagree for noisy data, complex anisotropic structure, or for the situation in which the initial polarization of the shear wave is close to a null direction (e.g., Long and van der Hilst, 2005a; Wüstefeld and Bokelmann, 2007; Vecsey et al., 2008). Second, a quality control and measurement quality ranking scheme was implemented, similar to the ranking scheme used by Long et al. (2009). Those splitting measurements with high SNR, good waveform clarity, elliptical initial particle motion, and linear (or nearly linear) corrected particle motion were classified as "good" as long as the measurement methods agreed within the 2σ error spaces and the individual measurement errors were less than $\pm 20°$ in fast direction and ± 0.6 s in delay time. Measurements with larger error bars (up to $\pm 35°$ in fast direction and ± 1.5 s in delay time), poorer waveform clarity, and less linear corrected particle motion were retained and classified as "fair" as long as the two measurement methods yielded consistent results (again, within the 2σ error spaces). Waveforms with linear or nearly linear initial particle motion were classified as null measurements; in the assessment of null measurement quality, noisier waveforms with lower SNR were classified as "fair," while high-quality waveforms were classified as "good." Properly defined, null measurements do not include noisy arrivals with poor waveform quality and only

Table 1
Summary of splitting results. Columns indicate the name and coordinates of the NARS-Baja stations and the number and quality of null and non-null splitting measurements.

Station	Latitude	Longitude	No. of nulls	No. of good (fair) nulls	No. of non-nulls	No. of good (fair) non-nulls
NE70	32.42095	−115.26078	6	1 (5)	6	2 (4)
NE71	31.68973	−115.90526	15	6 (9)	14	6 (8)
NE72	30.84843	−116.05857	4	0 (4)	2	1 (1)
NE73	30.0651	−115.34847	7	6 (1)	1	0 (1)[a]
NE74	28.00751	−114.0138	5	4 (1)	3	0 (3)
NE75	27.29334	−112.85649	30	23 (7)	0	0 (0)
NE76	26.88894	−111.99905	39	25 (14)	2	0 (2)
NE77	26.01578	−111.36133	32	20 (12)	5	1 (4)
NE78	24.3982	−111.10643	12	6 (6)	0	0 (0)
NE79	23.11937	−109.75611	15	6 (9)	7	1 (6)
NE80	30.5	−112.31993	21	13 (7)	0	0 (0)
NE81	28.91834	−109.63626	20	12 (8)	4	2 (2)
NE82	26.91566	−109.23084	7	6 (1)	7	3 (4)
NE83	24.73088	−107.73933	3	1 (2)	0	0 (0)

[a] Likely due to lower mantle anisotropy.

well-constrained nulls were classified as such in this study. Two typical examples of splitting analysis for the dataset presented here are shown in Fig. 3, including a non-null measurement and a null measurement.

4. Results

4.1. SKS splitting results

The data processing procedures described above yielded a total of 267 measurements, 216 of which were nulls. Of these, 169 were rated "good" quality; of the 51 non-null measurements, 16 were considered "good." Station NE76 had the highest number of measurements (41), but 39 of these were nulls. Station NE71 had the highest number of non-null measurements (14). The measurement procedures yielded, on average, 19 measurements per station, but several stations had considerably fewer (as few as 3). The number of measurements per station and their quality are summarized in Table 1.

Because of the preponderance of null measurements in the NARS-Baja splitting dataset, I first plot the individual nulls at the station location (Fig. 4); nulls are plotted as crosses, with the arms of the cross parallel to the backazimuth (equivalent to the incoming polarization azimuth for SKS waves) and the direction 90° from it. Most stations exhibit null splitting over a large range of backazimuths, and stations NE75, NE76, NE77, and NE80 exhibit clear nulls over the entire backazimuthal range. This behavior is consistent with either (near-) isotropy beneath the station, splitting that is smaller than the lower detection limit of the measurements or anisotropic structure that exhibits extreme lateral heterogeneity and is not coherent over the length scales associated with the seismic wavelengths under study. (At periods above 8–10 s, the splitting detection limit for broadband data with typical noise levels using the transverse component minimization or rotation-correlation measurement methods is ∼0.5 s; splitting with smaller delay times cannot typically be distinguished from the absence of splitting given the size of the measurement errors. For further details, see Long and Silver, 2009.) At several stations, most notably NE70, NE78, and NE82, the null directions cluster around a small range of backazimuths, which may be consistent with a simple anisotropic structure with the fast directions aligned along one of the null directions.

The "good" and "fair" non-null measurements obtained with the rotation-correlation and transverse component minimization methods are shown in Figs. 5 and 6, respectively. Because only those SKS arrivals for which the two methods agreed within the 2σ error spaces were retained in the dataset, the two maps are similar and differ only slightly in the details of individual measurements. Non-null measurements were only made at 10 of the 14 NARS-Baja stations. One non-null measurement was made at station NE73, but it is shown as a dashed line in Figs. 5 and 6; as discussed in Section 5.1, this measurement is likely contaminated by lower mantle anisotropy and probably does not reflect upper mantle anisotropy beneath the station. As Figs. 5 and 6 demonstrate, shear wave splitting patterns in the Gulf of California region are highly complex and variable, with adjacent stations often exhibiting drastically different splitting patterns (e.g., NE70 and NE71). Stations in the northernmost part of the array (NE70–NE72) tend to exhibit a relatively large amount of splitting, with delay times over ∼1 s and variable fast directions. Stations located along the central part of the Baja peninsula further to the south (NE75–NE78) are dominated by null measurements over a wide range of backazimuths and only a few non-null measurements; this is consistent with weak and/or complex anisotropy in the upper mantle. In the southern part of the array, several stations (NE77, NE79, NE81, and NE82) exhibit fast directions that are dominantly NE–SW. The level of complexity in the splitting patterns observed at NARS-Baja stations is comparable that in other studies of shear wave splitting in complex tectonic settings, including subduction zones (e.g., Fouch and Fischer, 1998; Long and van der Hilst, 2005b; Pozgay et al., 2007) and transform boundaries such as the San Andreas fault (e.g., Hartog and Schwartz, 2001; Polet and Kanamori, 2002).

4.2. Evidence for backazimuthal variations in splitting parameters

An important question in any SKS splitting study is whether there is evidence for well-constrained backazimuthal variations in splitting parameters at individual stations, which indicates that the local structure is more complex than a single horizontal layer of anisotropy. If backazimuthal variations are present but incompletely investigated, then single-station average splitting parameters based on a limited number of measurements may be misleading when they are interpreted in terms of mantle flow processes. Although the backazimuthal coverage in this dataset is not optimal and is heavily weighted towards events in the western Pacific Ocean (Fig. 2b), at many stations the 5 years' worth of data examined in this study afford sufficient backazimuthal coverage to investigate this question. Fig. 7 shows the variations of measured splitting parameters (using the rotation-correlation method) at stations NE82 and NE71. (Because the rotation-correlation and the transverse component minimization methods were found to yield very similar splitting results for this dataset, the choice of the rotation-correlation measurements for Fig. 7 and for subsequent calculations of average splitting parameters is arbitrary, but Fig. 7 would not look substantially different if the transverse component minimization method were used.)

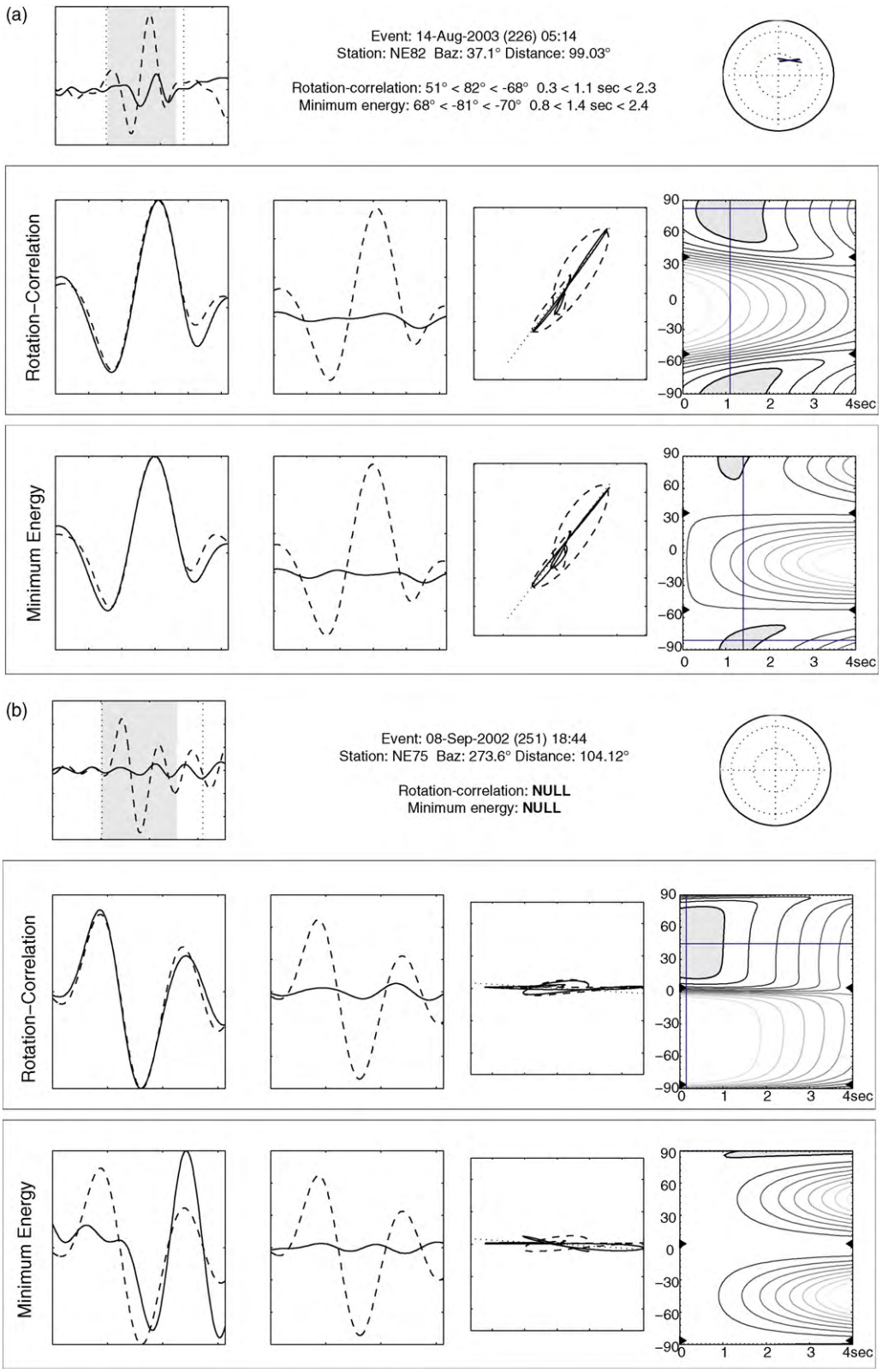

Fig. 3. Examples of splitting measurements of typical quality at NARS-Baja stations obtained using SplitLab (Wüstefeld et al., 2007). (a) Example of a non-null measurement at station NE82. Top left panel shows the uncorrected radial (dashed) and transverse (solid) components. The middle and bottom rows of panels show the diagnostic plots for the rotation-correlation method and the transverse component minimization method, respectively: from left to right, the corrected fast (dashed) and slow (solid) components, the corrected radial (dashed) and transverse (solid) components, the uncorrected (dashed) and corrected (solid) particle motion diagrams, and the error space maps. Both measurement methods yield similar results within the 2σ error spaces. (b) An example of a null measurement at station NE75. Diagnostic plots are as in part (a).

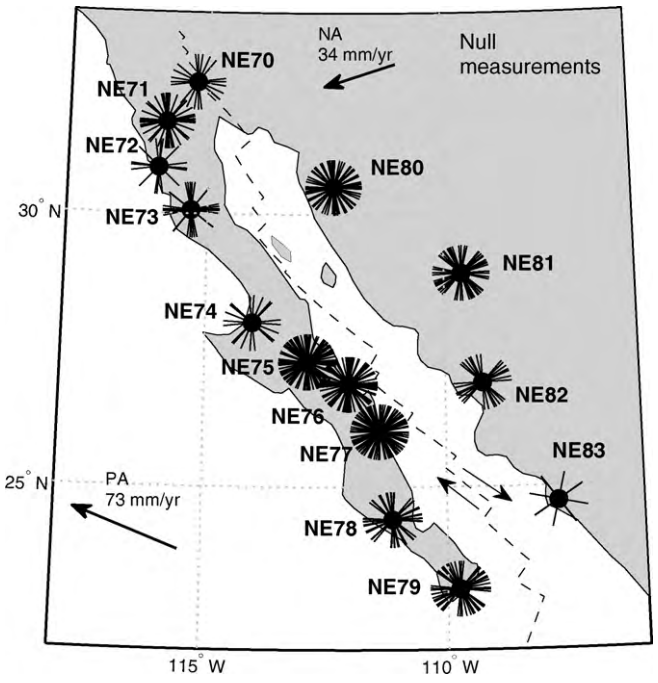

Fig. 4. Map of individual null measurements in the dataset. Nulls are plotted as crosses at the station locations, with the bars oriented in the direction of the SKS backazimuth and its orthogonal direction. The absolute plate motion directions of the North American (NA) and Pacific (PA) plates are shown with dark arrows, while the light arrows indicate the relative motion across the Gulf of California plate boundary (dotted line).

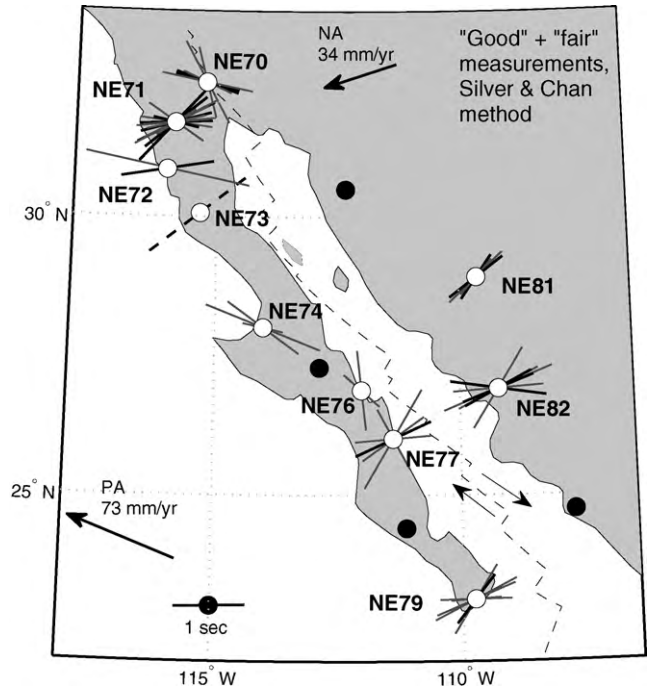

Fig. 5. Splitting map of all "good" and "fair" quality non-null measurements obtained using the Silver & Chan (1991) transverse component minimization measurement method, plotted at the station location. "Good" quality measurements are plotted as heavy black lines; "fair" measurements are plotted as light gray lines. The orientation and length of each bar corresponds to the fast direction and the delay time, respectively. The dotted line at station NE73 corresponds to a measurement that is likely contaminated by lower mantle anisotropy, as discussed in Section 5.1. Stations shown with black circles did not yield any well-constrained non-null splitting measurements. Absolute and relative plate motion and the location of the Gulf of California plate boundary are shown as in Fig. 4.

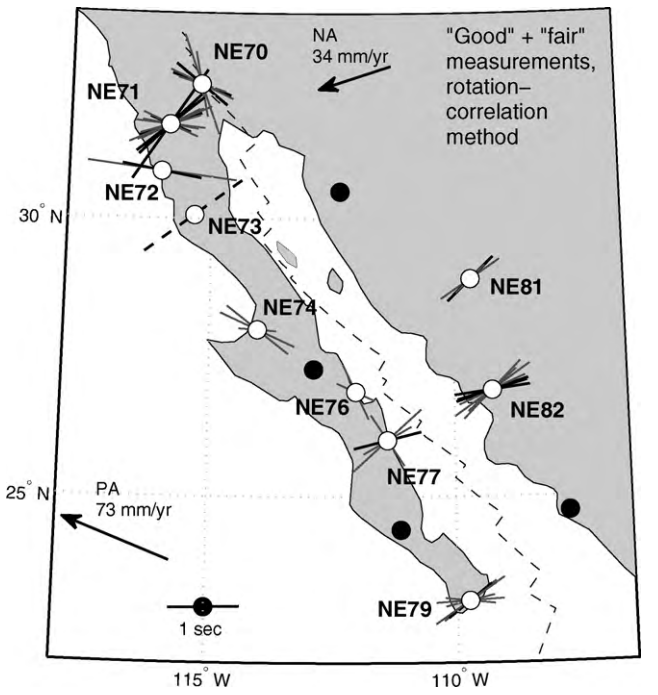

Fig. 6. Same as Fig. 6, but the measurements shown were obtained with the rotation-correlation (also known as cross-correlation) measurement method. A visual comparison with Fig. 5 indicates that discrepancies between the different measurement methods, while subtle, are not entirely negligible. These differences are likely due to the complex anisotropic structure beneath the region, as discussed in Section 5. Symbols are as in Fig. 5.

At station NE82 (Fig. 7a), there are no significant variations in measured splitting parameters with backazimuth, and the fast directions and delay times cluster around average values of $\phi = 80^\circ$, $\delta t = 1.3$ s. (It must be noted, however, that the backazimuthal coverage at this station remains somewhat limited.) At station NE71, shown in Fig. 7b, there is a distinctive dependence of measured ϕ values on backazimuth, with SKS arrivals coming from the northwest exhibiting NE–SW fast directions and arrivals from other directions exhibiting WNW–ESE fast directions. Unfortunately, the backazimuthal coverage at most stations in the dataset is not sufficient to carry out well-constrained forward modeling of these variations that invoke multiple anisotropic layers or dipping symmetry axes. Nevertheless, it is possible to classify each station as exhibiting backazimuthal variation in splitting (NE70, NE71, NE76, NE77, NE79, and NE82), exhibiting little or no variation (NE74, NE75, NE80, and NE81), or having insufficient backazimuthal coverage to make a determination (NE72, NE73, NE78, and NE83). The backazimuthal variation observed at many stations, along with the large number of null measurements over a large range of backazimuths observed at many stations that also have well-constrained non-null measurements, is a strong argument that the anisotropic structure beneath many stations in the Gulf of California region is generally complex and cannot be completely described by simple anisotropic models that invoke a single layer of horizontal anisotropy. This inference is also borne out by the observation of frequency-dependent SKS splitting, discussed in Section 4.4 below.

4.3. Comparison with previous splitting results

In order to compare the results obtained in this study with previous SKS measurements at NARS-Baja stations obtained by Obrebski et al. (2006) and van Benthem et al. (2008), I calculate average splitting parameters for 8 of the 14 stations by a simple averaging scheme (i.e., individual measurements were not weighted

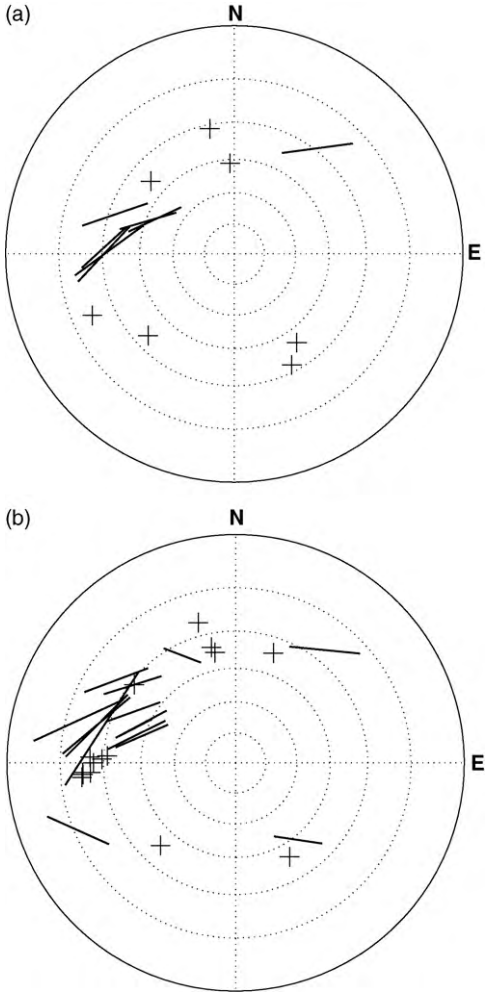

Fig. 7. Backazimuthal variation in measured splitting parameters (using the rotation-correlation method) for station NE82 (a) and NE71 (b). In each figure, individual measurements are plotted as bars with respect to backazimuth (azimuth around circle) and incidence angle (distance from center of circle; SKS arrivals in the dataset are nearly vertical and have incidence angles of less than 10°). Station NE82 (a) exhibits little variation of measured splitting parameters with event backazimuth; in contrast, station NE71 exhibits a more complicated splitting pattern (b).

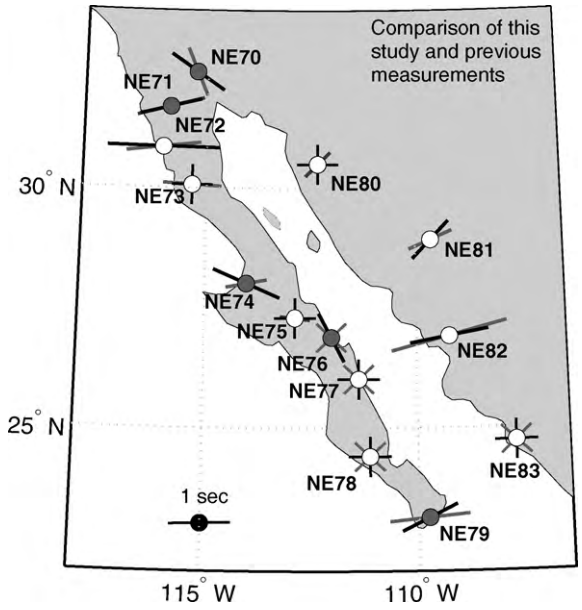

Fig. 8. Comparison of single-station average splitting parameters obtained using the low-frequency measurements presented in this study and those including higher-frequency energy obtained by Obrebski et al. (2006) and van Benthem et al. (2008). Black lines indicate results from this study and gray lines indicate results from previous studies. Thick lines indicate average splitting parameters (ϕ, δt) at those stations where averages were reported by previous studies (gray) or where physically meaningful averages could be obtained (black). Thin crosses indicate stations that are dominated by null measurements over a range of backazimuths (oriented at 0° and 90° in black, this study) or where some null measurements were obtained and no average splitting parameters were reported (oriented at 45° and 135° in gray, previous studies). Stations at which the splitting patterns exhibit significant complexity and/or variations in splitting parameters with backazimuth are shown with gray dots; at these stations, the physical meaning of the average splitting parameters must be evaluated with caution.

by the errors). (The Obrebski et al. and van Benthem et al. studies are hereinafter referred to as O2006 and B2008, respectively.) Of the remaining 6 stations, 4 exhibited only null measurements, NE77 exhibited a splitting pattern that was too complex to obtain a physically meaningful average, and the only non-null measurement obtained at NE73 was likely contaminated by lower mantle anisotropy (see Section 5.1). The average splitting parameters are plotted in Fig. 8, along with the station averages reported by O2006 and B2008. The average measurements are also shown in Table 2.

As Fig. 8 demonstrates, the results of this study are broadly consistent with previous measurements at many stations, most

Table 2
Average splitting parameters for NARS-Baja stations obtained in this study and in previous studies.

Station	Latitude	Longitude	phi, this study	dt, this study	phi, O2006/B2008	dt, O2006/B2008	Source
NE70	32.42095	−115.26078	−56°	1.1	−23°	0.9	O2006
NE71	31.68973	−115.90526	76°	1.1	75°	1.2	O2006
NE72	30.84843	−116.05857	91°	2.0	83°	1.3	O2006
NE73	30.0651	−115.34847	[a]	[a]	93°	1.0	O2006
NE74	28.00751	−114.0138	−66°	1.2	79°	0.7	O2006
NE75	27.29334	−112.85649	[a]	[a]	−83°	0.5	B2008
NE76	26.88894	−111.99905	−27°	1.0	[a]	[a]	B2008
NE77	26.01578	−111.36133	[b]	[b]	[c]	[c]	B2008
NE78	24.3982	−111.10643	[c]	[c]	[c]	[c]	B2008
NE79	23.11937	−109.75611	62°	1.0	84°	1.3	B2008
NE80	30.5	−112.31993	[a]	[a]	45°	0.6	O2006
NE81	28.91834	−109.63626	44°	0.9	66°	0.8	O2006
NE82	26.91566	−109.23084	79°	1.3	75°	2.0	B2008
NE83	24.73088	−107.73933	[c]	[c]	[c]	[c]	B2008

[a] Null measurements over a large range of backazimuths.
[b] Splitting pattern too complex to obtain physically meaningful average.
[c] Insufficient data; not enough measurements to obtain average or to rule out anisotropy.

Table 3
Individual measurements of frequency-dependent splitting for 8 SKS waveforms in the NARS-Baja splitting dataset. For each of these 8 SKS arrivals, well-constrained splitting parameters in both low (periods between ~10 and 50 s) and intermediate (periods between ~5 and 10 s) frequency bands were obtained. The columns indicate the station name, event day, latitude, and longitude, and the best-fitting splitting parameters (along with 95% confidence regions) at low and intermediate frequencies. The final column indicates whether the low- and intermediate-frequency measurements can be considered discrepant, given the size of the error bars.

Stat.	Event yyyy.jjj	Event lat	Event lon	Phi, low frequency	dt, low frequency	Phi, int. frequency	dt, int. frequency	Discrepant?
NE70	2003.133	−17.29	167.74	88 < −71° < −46	0.6 < 1.0 < 1.6	−68 < −55° < −50	0.9 < 1.2 < 1.4	N
NE70	2003.146	6.76	123.71	NULL	NULL	−27 < −8° < 1	0.6 < 0.8 < 1.1	Y
NE71	2002.161	10.98	140.69	43 < 62° < 82	1.0 < 1.3 < 1.6	37 < 44° < 64	0.6 < 0.8 < 1.0	Y
NE71	2003.182	12.80	124.90	70 < 87° < −84	0.9 < 1.1 < 1.6	−90 < −87° < −88	2.3 < 2.5 < 2.7	Y
NE71	2004.204	26.49	128.89	60 < 74° < −92	0.9 < 1.1 < 1.4	72 < 80° < −92	1.1 < 1.3 < 1.5	N
NE71	2005.017	10.99	140.68	35 < 42° < 56	1.2 < 1.6 < 2.0	46 < 60° < 78	0.6 < 0.8 < 1.0	Y
NE82	2003.226	39.16	20.60	68 < −81° < −70	0.8 < 1.4 < 2.3	80 < 81° < 86	1.4 < 1.5 < 1.6	N
NE82	2005.046	4.76	126.42	39 < 68° < −90	0.7 < 1.1 < 1.7	86 < 88° < −92	1.8 < 2.0 < 2.1	Y

notably NE71, NE72, NE81, and NE82. However, there are a few significant discrepancies between the dataset presented here and previous studies. At station NE76, for example, I identified nearly a second of splitting with an average fast direction of N25°E, while B2008 identified only null splitting for several backazimuths. At other stations, such as NE70, NE74, and NE79, there are significant discrepancies between the average splitting parameters obtained in this study and those obtained by previous workers (Table 2). At stations NE73 and NE75, I identified only null measurements, while O2006 obtained well-constrained splitting parameters. At station NE75, this discrepancy can be explained by the fact that the average delay time obtained by O2006 is 0.5 s, which is near the lower detection limit for periods greater than 8–10 s for the measurement methods used in this study. The reason for the discrepancy at NE73 is less clear.

What could be the explanation for the discrepancies documented in Fig. 8 and Table 2? One difference between the dataset presented here and those presented in previous studies is that it covers a longer time period (5 years of data as opposed to 2–3). In the presence of complex anisotropic structure that could cause backazimuthal variations in splitting, it is possible that a larger dataset that covers a longer time period may result in slightly different average splitting parameters at individual stations. It is unlikely, however, that this accounts for all the differences shown in Fig. 8. The other major difference between this study and the work of O2006 and B2008 is the frequency content of the waves under study. Here, I have focused on the long-period part of the SKS signal, and filtered out energy at frequencies higher than 0.1 Hz (this corner frequency was occasionally adjusted to 0.125 Hz to improve the clarity of individual waveforms, but 0.1 Hz was used for most arrivals in the dataset). O2006 and B2008 used a filtering scheme that retained energy at periods between ~1 and ~25 s and therefore included SKS energy at higher frequencies. It is likely that many of these SKS arrivals were dominated by energy at periods shorter than the ~10 s cutoff used in this study; for example, the sample waveform shown in O2006 (see supplementary information to Obrebski et al., 2006) has a characteristic period of ~5 s. It is likely, therefore, that some of the discrepancies between the results presented here and previous studies are due to the dependence of measured splitting parameters on frequency. Such a frequency dependence has been established in other studies of teleseismic and local shear wave splitting due to upper mantle anisotropy, including in Australia (Clitheroe and van der Hilst, 1998), New Zealand (Marson-Pidgeon and Savage, 1997; Greve et al., 2008), the Marianas (Fouch and Fischer, 1998), and Japan (Long and van der Hilst, 2005a; Wirth and Long, 2010).

4.4. Results of frequency dependence tests

In order to investigate further the frequency dependence suggested by the comparison presented in Section 4.3, the highest-quality SKS arrivals that showed evidence of splitting at periods greater than 10 s were identified in the dataset and were subjected to a series of bandpass filters and additional splitting measurements. This approach allows for the identification of frequency-dependent splitting in individual waveforms. In addition to testing the highest-quality SKS waveforms in the dataset, I examined the individual splitting measurements reported in O2006 and B2008 and compared them to my dataset in order to identify individual event–station pairs with significant discrepancies. Only 16 SKS arrivals were identified as having well-constrained measurements in both this study and one of the previous studies. Of the 16 SKS arrivals in common between this dataset and O2006 or B2008, 5 can be labeled as discrepant, but 2 of the measurements in question in the B2008 dataset had error bars on δt larger than the δt value itself and may not be well constrained. The remaining 3 discrepant SKS arrivals were also examined for evidence of frequency-dependent splitting.

It is important to note that characterizing frequency-dependent shear wave splitting due to upper mantle anisotropy using only SKS arrivals is difficult, as SKS waves usually are dominated by energy at relatively long periods (typically greater than ~8 s) and many arrivals have little energy at higher frequencies. Many studies which have documented frequency-dependent shear wave splitting have relied on local S phases, which typically display more high-frequency energy (e.g., Marson-Pidgeon and Savage, 1997; Fouch and Fischer, 1998; Greve et al., 2008; Wirth and Long, 2010). A variety of factors will influence the frequency content of shear phases (e.g., Carter and Kendall, 2006), most notably the attenuation structure along their mantle raypaths, and the amount of high-frequency energy present in the SKS arrivals in the Nars-Baja dataset therefore varies for different event–station pairs. Despite these difficulties, however, the procedure described above yielded a total of 8 SKS arrivals for which well-constrained splitting measurements could be made both at "low" frequencies (periods greater than 10 s) and "intermediate" frequencies (periods between 4–5 and 10 s). An attempt was made to measure SKS splitting at "high" frequencies (periods less than ~5 s), but in general, there was very usable SKS energy at these periods, and the comparison is therefore limited to periods greater than 5 s. The results of these frequency tests are shown in Table 3 and two examples of intermediate and low-frequency splitting measurements are shown in Fig. 9; one example exhibits consistent splitting and the other exhibits discrepant splitting. Of the 8 SKS phases that were examined for a frequency effect, 5 exhibited frequency-dependent splitting, while splitting parameters were found to be independent of frequency at the remaining 3. The dependence of δt on frequency for the 5 frequency-dependent arrivals is shown in map view in Fig. 10. Interestingly, in all cases the measured ϕ values were found to be independent of frequency; only the delay times were affected by the frequency content. The effect of frequency on δt was not uniform, however; in 3 of the 5 cases, higher-frequency measurements produced higher delay times, but this effect was reversed for the other 2 arrivals. The frequency tests shown in Figs. 9 and 10 and

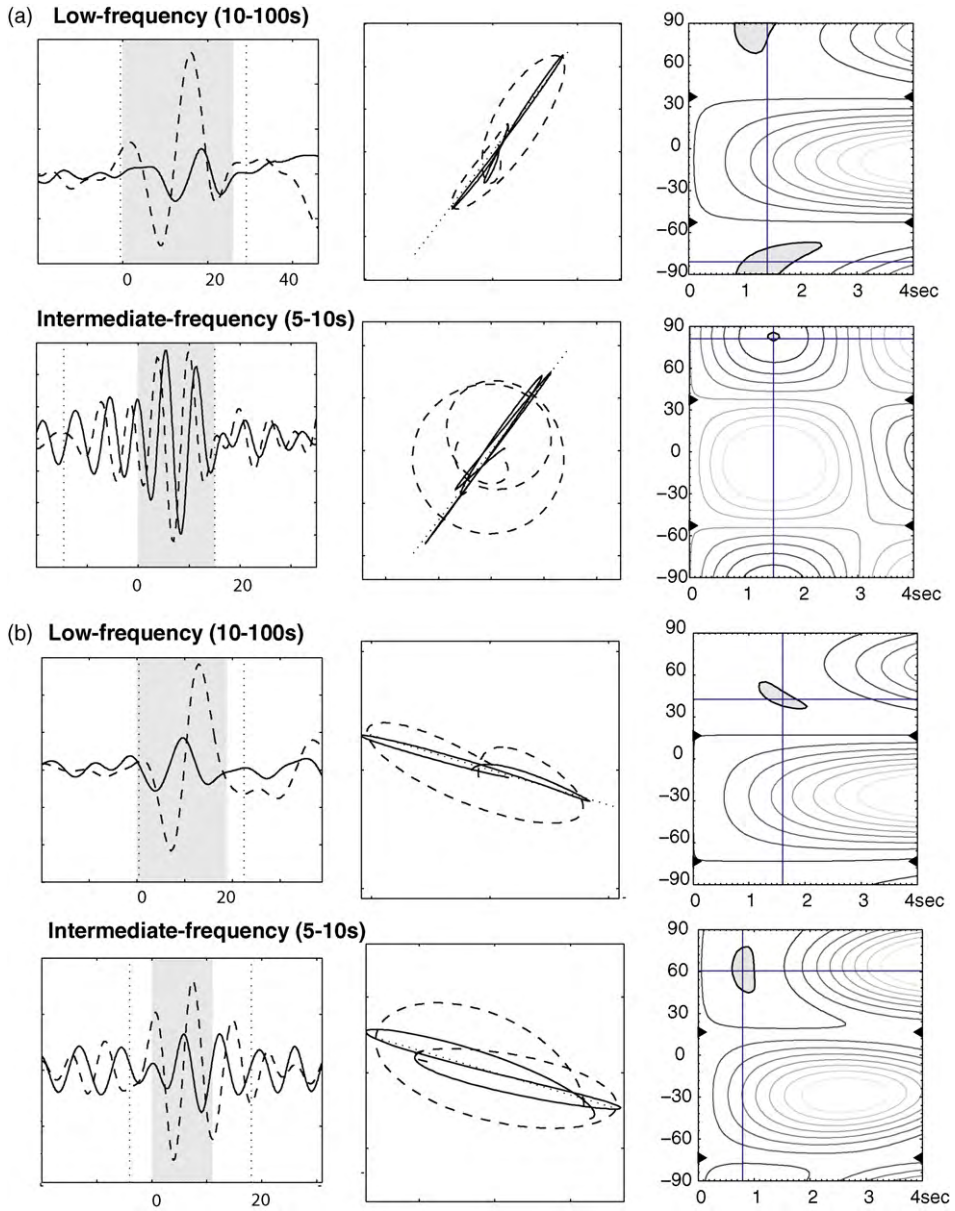

Fig. 9. Example of frequency dependence for two sets of SKS waveforms. (a) Example of an SKS arrival that does not exhibit frequency-dependent splitting. The example shown is from station NE82 for an event located in the Mediterranean region (2003.226.05:14). At periods between 10 and 100 s (top row), the Silver and Chan (1991) method yields splitting parameters of ϕ: 68° < −81° < −70°; δt: 0.8 < 1.4 < 2.4 s. From left to right, the radial (dotted) and transverse (solid) components are shown (left panel; time shown on x axis in seconds), along with the uncorrected (dotted) and corrected (solid) particle motion diagrams (middle panel) and the error space plot (right panel). At periods between 5 and 10 s (bottom row), the measurement yields similar (but better-constrained) parameters of ϕ: 80° < 81° < 86°; δt: 1.4< 1.5 < 1.6 s. (b) An example of an SKS arrival that does exhibit frequency-dependent splitting. This example is from station NE71 for an event located in the southern Marianas (2005.017.10:50). At lower frequencies (periods between 10 and 100 s), the measured splitting parameters are ϕ: 35° < 42° < 56°; δt: 1.2 < 1.6 < 2.0 s. At higher frequencies (periods between 5 and 10 s), the measured splitting parameters are ϕ: 46° < 60° < 78°; δt: 0.6 < 0.8 < 1.0 s. As demonstrated as the plots of the error surfaces (right panels), the 2σ error surfaces for the two measurements do not overlap.

Table 3, along with the discrepancies between the results of this study and previous SKS splitting studies in the region shown in Fig. 8, provide evidence for frequency-dependent shear wave splitting in the Gulf of California, although the effect is limited to delay time measurements.

5. Discussion

5.1. Possible contributions from lower mantle anisotropy

It is usually assumed that SKS splitting is mainly due to upper mantle anisotropy beneath the receiver and that any contribution from anisotropy in the lower mantle is negligible. This assumption is based on seismological and experimental evidence that much of the lower mantle is isotropic (e.g., Meade et al., 1995) and on the observation that SKS and SKKS phases, which have similar raypaths in the upper mantle but whose paths diverge significantly in the lower mantle, exhibit similar splitting approximately in 95% of cases (e.g., Niu and Perez, 2004). However, a few studies have identified discrepancies between SKS and SKKS splitting for the same event–station pairs and have attributed this to anisotropy in the lower mantle far away from the receiver. Recently, Long (2009) observed large discrepancies between SKS and SKKS splitting at NARS-Baja stations and neighboring stations in Mexico and Cali-

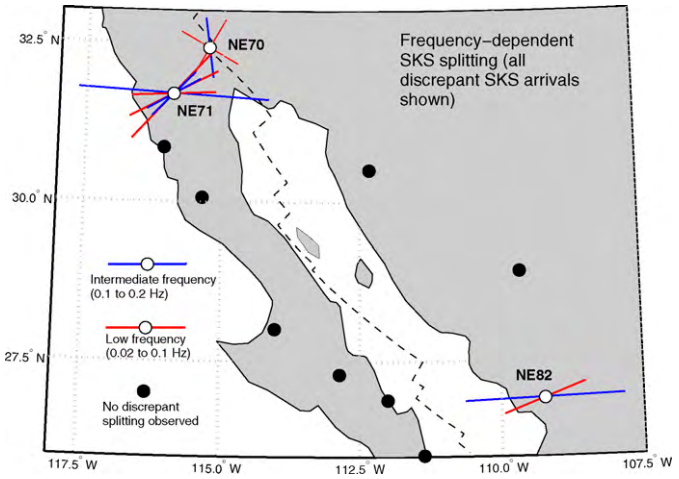

Fig. 10. Frequency-dependent SKS splitting shown in map view. The five SKS arrivals which exhibited discrepant low- and intermediate-frequency splitting in the tests described in Section 4.4 are shown; intermediate frequency measurements are shown in blue, while low frequency measurements are shown in red. The thin red lines at station NE70 depict a low-frequency null measurement. The scale bars indicate 1 s of delay time. (For interpretation of the references to color in this figure legend, the reader is referred to the web version of the article.)

fornia for a group of events located in the western Pacific. These observations were attributed to a region of anomalous anisotropy in the D" layer beneath the eastern Pacific off the west coast of North America (Long, 2009). Although the anomalous anisotropy was found mainly to affect SKKS phases and not the corresponding SKS phases, the question of whether the dataset presented here could be contaminated by anisotropy in the lower mantle remains important. The anomalous splitting attributed to lowermost mantle anisotropy by Long (2009) exhibited delay times between 1 and 3 s and fast directions that clustered closely around an average value of $\phi \cong 50^\circ$ and was associated with arrivals from a group of events in the western Pacific with backazimuths between ~270° and 290°. A key question, therefore, is whether any of the NARS-Baja stations exhibit SKS splitting that is consistent with the lower mantle anisotropy inferred by Long (2009).

Three of the stations (NE73, NE81, and NE82) exhibit splitting that is dominated by fast directions near ~50°. At NE82, there are consistent measurements from several different backazimuths, so the signal is unlikely to be due to lower mantle anisotropy. At NE81, several well-constrained SKS splitting measurements with delay times ranging from 0.7 to 1.1 s were made; these δt values are considerably smaller than most of the D"-associated SKKS delay times found by Long (2009). A contribution from the lower mantle cannot be ruled out at this station, but it is difficult to argue that the all of the SKS splits observed at NE81 are due to the previously identified D" anomaly. I conclude that the splitting observed at NE81 is most likely due to upper mantle anisotropy beneath the station, but its interpretation should be treated with some caution. Station NE73 exhibited well-constrained null measurements over a range of backazimuths and only a single non-null measurement ($\phi = 51^\circ$, $\delta t = 1.9$ s) was identified at this station. These SKS splitting parameters are quite consistent with the splitting associated with lower mantle anisotropy identified by Long (2009) and the event is located off Papua New Guinea, in the zone of events that is inferred to produce anomalous lower mantle splitting. It is therefore likely that this SKS phase has been contaminated by lower mantle anisotropy and cannot be unambiguously attributed to processes in the upper mantle; the measurement is shown as a dotted line in Figs. 5 and 6 and is not included in Fig. 8 or in the subsequent interpretation.

5.2. A mechanism for frequency dependence

Frequency-dependent shear wave splitting has been identified in a variety of regions and tectonic settings, and several theories have been proposed to explain the frequency dependence. In an exploration geophysics setting, it has been proposed that anisotropy due to porous flow through fractured reservoirs can produce frequency-dependent splitting and that this frequency dependence can be used to estimate fracture size (Liu et al., 2003). Similarly, models that invoke aligned partial melt have been proposed to explain frequency-dependent splitting beneath the North Island of New Zealand (Greve et al., 2008); in this type of model, the spacing between aligned bands of melt controls the wavelengths over which the shear waves will be sensitive to the anisotropy induced by shape-preferred orientation. Waveform modeling studies have also shed light on the problem of frequency-dependent splitting: for example, Saltzer et al. (2000) demonstrated that in the presence of anisotropy whose geometry varies with depth, higher-frequency energy is biased towards the near-surface layers and the measured apparent splitting parameters will depend on frequency. Work by Rümpker et al. (1999) on frequency-dependent splitting in the presence of depth-dependent anisotropy indicates that longer-period measurements may be less sensitive to the presence of sharp anisotropic gradients. This study established that shear wave splitting estimates will depend on the filtering scheme used if anisotropy varies with depth and, conversely, that frequency-dependent splitting likely indicates depth-dependent anisotropic structure (Rümpker et al., 1999).

The interpretation of shear wave splitting parameters is often considered in a ray theoretical framework, but the abundant observations of frequency-dependent shear wave splitting makes the need to consider finite-frequency effects obvious. Simple calculations of the width of the first Fresnel zones for shear waves at different characteristic periods can be used to approximate the finite-frequency sensitivity of splitting measurements (e.g., Alsina and Snieder, 1995). Recently, more precise methods for computing the finite-frequency sensitivity of shear wave splitting measurements have been developed (e.g., Favier and Chevrot, 2003; Favier et al., 2004; Long et al., 2008) and as these and similar studies demonstrate, the sensitivity of teleseismic splitting measurements is highly dependent on frequency. In particular, Long et al. (2008) showed that finite-frequency sensitivity kernels can be extremely complex when computed in realistic, heterogeneous background models. Such finite-frequency effects provide the most likely explanation for the frequency-dependent splitting observed in the Gulf of California region. SKS waves with different frequency contents will sample upper mantle anisotropy in a different way, and finite-frequency effects can be complicated and non-intuitive for realistically heterogeneous background models (Long et al., 2008). In the presence of complex anisotropy that varies laterally and/or with depth, this effect can induce a dependence of measured splitting parameters on frequency. In the case of the NARS-Baja dataset, the frequency dependence is observed in the delay time measurements but not in the fast directions. This suggests that the strength of anisotropy is heterogeneous and varies with depth, laterally, or both.

5.3. Depth distribution of anisotropy

In order to properly interpret shear wave splitting measurements in terms of dynamic processes at depth, it is important to consider the likely depth distribution of the anisotropic structure and whether the relative contribution of anisotropy in the crust, the mantle lithosphere, and the asthenosphere to the observed splitting signal can be distinguished. This exercise can be particularly difficult in the presence of complex splitting such as those observed

in the Gulf of California region, but a few first-order inferences can be made. A first question is whether there is likely to be a large contribution to the observed splitting from crustal anisotropy. There are few constraints on crustal splitting in this area, but Zúñiga et al. (1995) and González and Munguía (2003) examined splitting from crustal earthquakes in the Mexicali Valley and Cerro Prieto Fault area (to the east of station NE70). Zúñiga et al. (1995) identified delay times ranging up to 0.3 s and González and Munguía (2003) found up to 0.5 s of crustal splitting (average value ~0.35 s) consistent with stress-aligned cracks in the upper crust. These measurements were undertaken at high frequencies (up to 40 Hz), however, and it is unclear whether crack-induced anisotropy in the upper crust would have a large effect on SKS waveforms with characteristic periods of ~10 s. Because available observations of crustal anisotropy are geographically limited, arguments about the contribution of crustal anisotropy to the measurements presented here remain indirect. Most workers have argued that the crust generally contributes less than ~0.3 s of splitting to SKS-type measurements (e.g., Silver, 1996), but very small-scale lateral variations in SKS splitting, for example, may not be explicable in terms of mantle anisotropy and likely require a contribution from the crust (see, e.g., Long and Silver, 2009, and references therein). It is likely that crustal anisotropy makes a small contribution to the low-frequency SKS splitting measurements presented here, but it is unlikely that shallow crustal anisotropy such as that inferred by González and Munguía (2003) represents the primary contribution to the ~1 s of splitting or more observed at long periods at some NARS-Baja stations.

A second line of argument that there is a significant contribution from mantle anisotropy comes from the phase velocity maps of Zhang et al. (2007, 2009), who measured Rayleigh wave dispersion for the Gulf of California region. These studies identified significant 2ψ azimuthal anisotropy at periods of ~50 s and longer, which are primarily sensitive to mantle structure. These results argue that there is likely significant anisotropy at upper mantle depths beneath the Gulf of California region and imply that particularly for NARS-Baja stations that exhibit splitting of ~1 s or more, a large part of the splitting signal observed in this study must be due to mantle anisotropy. A more detailed comparison between the SKS splitting results presented here and the surface wave results of Zhang et al. (2007, 2009) can be found in Section 5.4.

As discussed by Obrebski et al. (2006) and others, a key issue in interpreting SKS splitting is distinguishing between present-day mantle deformation in the asthenosphere and "frozen" anisotropy in the rigid mantle lithosphere that is a consequence of past tectonic deformation episodes. Given the complexity in the NARS-Baja splitting dataset, it is very likely that both crustal/lithospheric anisotropy and asthenospheric anisotropy make a contribution to the observed splitting signal. It has been argued that the mantle lithosphere beneath the Gulf of California region is thin or nonexistent (Obrebski et al., 2006), based on the very low upper mantle velocities (e.g., Lebedev and van der Hilst, 2008; Nettles and Dziewonski, 2008) and on the supposition that the mantle lithosphere beneath westernmost North America was largely removed by low-angle Laramide subduction (e.g., Bird, 1988). If the mantle lithosphere in this region is indeed thin, then splitting measurements at stations that exhibit relatively large delay times (NE70, NE71, NE72, NE74, NE79, NE82) are most likely reflecting a contribution from present-day flow in the asthenosphere.

5.4. Comparison with surface wave anisotropy.

A direct quantitative comparison of surface wave azimuthal anisotropy and shear wave splitting for this region is difficult, since Zhang et al. (2007, 2009) only present azimuthally anisotropic phase velocity maps and do not invert directly for the depth distribution of anisotropy. However, a qualitative comparison between the splitting and surface wave models is possible. Phase velocity maps of at periods of 50–100 s are most relevant for this comparison, since these periods are primarily sensitive to upper mantle anisotropy. Notably, I do not find a striking correspondence between the SKS splitting measurements described in this study and the phase velocity maps of Zhang et al. (2009; see Fig. 4). Qualitatively, the Zhang et al. (2009) model would tend to predict weak splitting with a NW–SE fast direction at stations to the east of the Gulf of California. This is consistent with the null splitting observed at station NE80 (Fig. 4), but inconsistent with the generally NE–SW fast directions observed at stations NE81 and NE82 (Fig. 6). For stations located on the Baja Peninsula, the surface wave model would tend to predict generally E–W fast splitting directions in the north with more NW–SE-directed fast directions in the middle part of the peninsula and weaker splitting to the south. Again, this is not obviously consistent with the splitting observations (Figs. 4 and 6). I emphasize, however, that this comparison is necessarily qualitative and that a quantitative comparison between the surface wave model of Zhang et al. (2009) and the splitting observations documented here would be crucial for a full understanding of the complex anisotropic structure beneath the Gulf of California region. Such a comparison would require a fully 3D inversion of Rayleigh wave dispersion data for azimuthal anisotropy, however, and is beyond the scope of this paper.

5.5. Relationship between splitting and mantle flow

In order to properly relate the measured splitting due to upper mantle anisotropy to mantle flow processes, it is important to identify the mechanism for generating upper mantle anisotropy in a given region and to understand the geometrical relationship between mantle flow and the resulting anisotropy. Upper mantle anisotropy can be generated either through the LPO of its constituent minerals, primarily olivine, or through the SPO of elastically distinct material such as melt. It has been suggested that melt-related SPO might control anisotropy in the vicinity of continental rifts (e.g., Vauchez et al., 2000), so the possibility of SPO-generated anisotropy must be considered here. While it is likely that significant partial melt is present in the upper mantle immediately beneath the active rift segments (e.g., Lizzaralde et al., 2007) it is less likely that there is ubiquitous partial melt in the upper mantle everywhere in the Gulf of California region, and at stations located far from the rift center, upper mantle anisotropy is more likely to be controlled by the LPO of olivine. If deformation beneath the region is occurring in the A-, C-, or E-type olivine regime, then the fast direction of splitting should roughly correspond to the local direction of (horizontal) mantle flow beneath the station (e.g., Karato et al., 2008, and references therein). In contrast, the presence of B-type olivine fabric would imply that the flow direction should be offset from the fast direction by 90°. Laboratory investigations of the olivine fabric diagram have demonstrated that the type of fabric is sensitive to water content as well as temperature and stress and that B-type olivine fabric is associated with the presence of water, low temperatures, and high stresses (Karato et al., 2008, and references therein). The relatively high upper mantle temperatures beneath the Gulf of California region inferred from tomographic inversions (e.g., Zhang et al., 2007, 2009; Lebedev and van der Hilst, 2008; Wang et al., 2009) would imply that the conditions needed for B-type olivine fabric are unlikely to be present. Recent experimental work by Jung et al. (2009) has provided some evidence for a pressure-induced transition from A-type to B-type olivine fabric, but the applicability of these experiments to mantle conditions has not yet been established, and the depth range over which such a transition might take place at realistic deviatoric stress levels is not yet well understood. Therefore, in my subsequent interpreta-

tion I assume that the portion of the splitting signal which can be attributed to upper mantle anisotropy can be interpreted in terms of A-, C-, or E-type olivine LPO.

5.6. Mantle flow beneath the Gulf of California region

The splitting dataset presented here is complex, with frequency-dependent splitting, small-scale lateral variations in splitting behavior, and well-constrained backazimuthal variations in splitting at several stations. The fact that non-null splitting measurements often coexist at a given station with well-constrained null measurements over a large swath of backazimuths (e.g., station NE77; see Figs. 4–6) is a further indication of complicated anisotropic structure at depth. The frequency-dependent splitting observed in this dataset is an indication of vertical heterogeneity in anisotropic structure, and the lateral variations in splitting behavior (often over short length scales) is an indication of lateral heterogeneity. The level of complexity in splitting patterns observed at NARS-Baja stations is comparable to that observed in other splitting datasets in tectonically complex regions (e.g., Japan: Long and van der Hilst, 2005b; Wirth and Long, 2010).

Despite the complexity of the dataset in general, several stations exhibit strong, relatively well-constrained splitting that can be related to the tectonic setting. In the north, station NE70 exhibits a relatively simple splitting pattern with average splitting parameters of $\phi = -56^\circ$, $\delta t = 1.1$ s. The fast direction here is parallel to the strike of the transform plate boundary, and may be controlled by simple shear between the North America and Pacific plates (see also Obrebski et al., 2006). The delay time of 1.1 s is too large to be explained only by crustal anisotropy and requires a significant contribution from the mantle. The splitting pattern at station NE71 is complex, and this station may mark a transition from plate-boundary-parallel strain beneath station NE70 to the roughly E–W fast direction observed at station NE72. This E–W fast direction is oblique to both the absolute motion of the Pacific Plate (Fig. 1) and to the relative motion of the Pacific and North American plates, and may be best interpreted as a result of localized mantle upwelling beneath the Wagner basin, as discussed below. Although the average splitting parameters for this station (Fig. 8 and Table 2) are based on only two measurements, they come from two disparate backazimuths, they are both well-constrained, and the delay times are large, which argues for contemporary asthenospheric mantle flow in an E–W direction beneath NE72.

The group of stations located beneath the central portion of the Baja Peninsular Range (NE74–NE78) tend to be dominated by null measurements over a wide range of backazimuths (Fig. 4), and this argues for near-isotropy in the mantle beneath this region, nearly vertical mantle flow which would not produce significant splitting of SKS waves, or highly complex anisotropic structure which is not coherent over large length scales (or for a combination of these effects). Because stations NE74 and NE76 exhibit a few non-null measurements in addition to the large number of nulls, the latter scenario seems most likely. The average fast directions at NE74 and NE76 are roughly parallel to the transform plate boundary, but they must be interpreted with caution because they are accompanied by a large number of well-constrained nulls. As discussed further below, the region of inferred complex anisotropy beneath stations NE74–NE77 coincides geographically with the inferred location of stalled fragments of the Guadalupe microplate, which may be controlling the anisotropic structure of the upper mantle.

To the east of the rift, splitting behavior at stations NE80–NE83 can be split into two categories: stations which exhibit null splitting measured at several different backazimuths (NE80 and NE83, although only 3 measurements are available at the latter station) and those that are dominated by roughly ENE–WSW fast directions (NE81 and NE82). These are roughly parallel to the absolute motion of the North American plate, and it is likely that the anisotropy beneath NE81 and NE82 is controlled by absolute plate motion (APM)-parallel flow in the asthenosphere. In this context, however, the null splitting observed at NE80 and NE83 is puzzling, since one might expect these stations to have a similar splitting signature. While the data are very limited at NE83, station NE80 exhibits clear null splitting over a range of backazimuths. It may be that there is an additional contribution from the crust and/or mantle lithosphere that cancels out the effect of APM-parallel mantle flow at station NE80, or the mantle beneath NE80 may be dominated by vertical mantle flow associated with a buoyant, melt-rich upwelling, as discussed below.

The first-order observation that upper mantle anisotropy beneath the Gulf of California is complex and heterogeneous is likely a consequence of its recent tectonic history; the tectonic setting (and presumably the associated mantle flow field) has undergone a complete reorganization over the past ~12 Ma. The splitting behavior observed at NARS-Baja stations is considerably more complicated than that observed at stations located near mature continental rifts, which usually exhibit fast directions that are parallel (or oblique) to the strike of the rift (e.g., Gao et al., 1997). The observation that anisotropy beneath the Gulf of California is much more complicated than that inferred beneath mature continental rifts is significant: it may reflect the more complex kinematics of the Gulf of California rift zone (i.e., short segments of oblique rifting connected by long transform faults), or it may be a consequence of the reorganization of the mantle flow field from that associated with relatively recent Farallon subduction to that associated with present-day oblique rifting. One possibility is that this reorganization of the mantle flow field requires a longer time to complete than the ~12 Ma since the cessation of subduction and the subsequent localization of strain along the rift at ~5 Ma (Oskin et al., 2001). A second possibility is that this reorganization of the mantle flow field has been hindered by a stalled fragment of the Guadalupe microplate, itself a remnant of the Farallon plate. Several studies have argued that there is seismological evidence for such a stalled fragment (e.g., Michaud et al., 2006); lines of evidence for this include a region of relatively high shear velocities at 120–160 km depth beneath the south-central part of the Baja peninsula (Zhang et al., 2007, 2009) and anomalous P-to-S conversions in this region from receiver function analysis (Persaud et al., 2007; Obrebski and Castro, 2008). The region of the velocity anomaly identified by Zhang et al. (2009) coincides geographically with the region of the Baja peninsula dominated by complex splitting patterns and/or null splitting measurements (stations NE74–NE78; Figs. 4–6). A plausible scenario, therefore, is that the fragment of Farallon slab that has become lodged in the upper mantle beneath the Gulf of California has inhibited the large-scale reorganization of mantle flow, resulting in the complex and heterogeneous splitting observed at NARS-Baja stations.

Recently, Wang et al. (2009) suggested that mantle flow in the Gulf of California region might be controlled by a series of buoyant mantle upwellings spaced approximately 250 km apart based on the observation of low-velocity anomalies in the uppermost mantle in the vicinity of (though not directly beneath) the rift zone. This model, which invokes a dynamic component of upwelling induced by either the retention of buoyant melt or by depletion of the mantle matrix during melting, would predict predominantly vertical mantle flow directly beneath the velocity anomalies and would likely be associated with some component of horizontal mantle flow away from each upwelling center. For the northern stations in the NARS-Baja array, the splitting patterns appear to be consistent with the predictions of this model. Station NE80, which exhibits null splitting over a range of backazimuths, is located just at the edge of the presumed Delfin Basin upwelling (Figs. 4 and 11), while the fast directions observed at sta-

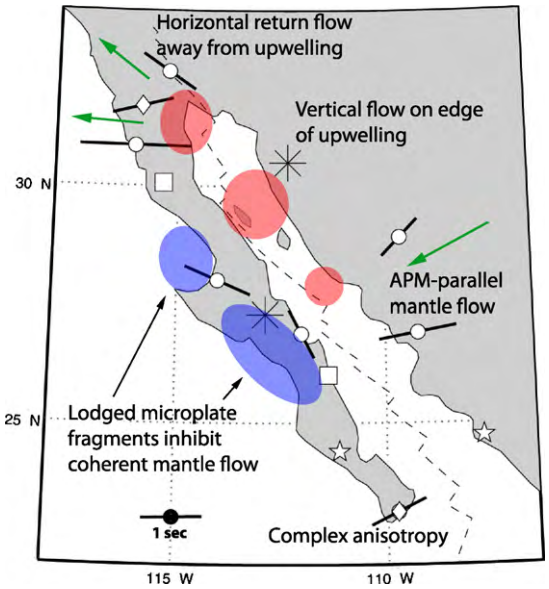

Fig. 11. Sketch of preferred flow model to explain the NARS-Baja splitting results. Average fast directions and delay times (black lines) are shown at those stations where the splitting pattern is simple enough to obtain a physically meaningful average that can be interpreted in terms of mantle flow. Stations dominated by null splitting are shown with crosses; stations with insufficient data quality or quantity are shown with starts. Stations marked with a square had splitting patterns that were ambiguous or too complex to obtain a physically meaningful average. At stations marked with a diamond, there was notable backazimuthal dependence of splitting parameters, and while average splitting parameters are shown, they should be treated with some caution. Green arrows mark the inferred direction of horizontal mantle flow. Zones of upwelling as proposed by Wang et al. (2009) are shown with red ellipses, while locations of the proposed microplate fragments lodged in the upper mantle are shown as blue ellipses. (For interpretation of the references to color in this figure legend, the reader is referred to the web version of the article.)

tions NE70, NE71, and NE72, which are adjacent to the presumed Wagner Basin upwelling, are generally consistent with horizontal return flow away from the upwelling center. In contrast, stations NE75, NE76, and NE77, which are adjacent to the inferred Guaymas Basin upwelling, exhibit highly complex splitting patterns which are dominated by null measurements and do not appear to be consistent with horizontal mantle flow away from the upwelling center. Instead, coherent mantle flow in this region appears to be inhibited by the lodged fragments of the Guadalupe microplate, resulting in complex, mainly null splitting, as described above.

My preferred model for mantle flow in the Gulf of California region is summarized in Fig. 11, and incorporates the competing effects of APM-parallel flow, the flow associated with melt-induced upwellings beneath the rift, and the stalled fragments of the Guadalupe microplate. Of the four NARS-Baja stations located to the east of the rift zone, it appears as though two of them (NE81 and NE82) overlie mantle that is dominated by APM-parallel flow, while beneath NE80 the flow field appears to be dominantly vertical, as it is located on the edge of what was inferred to be a mantle upwelling beneath the Delfin Basin by Wang et al. (2009). At station NE83, the data are of insufficient quality to determine the character of mantle flow. At the northern end of the Gulf, splitting at stations NE70–NE72 is generally consistent with horizontal flow away from the northernmost upwelling centered in the Wagner Basin, although the complex splitting patterns observed at NE70 and NE71 indicate multiple layers of anisotropy, with a likely contribution from lithospheric structure. Beneath the central part of the Baja Peninsula, splitting patterns are complex and heterogeneous, which are consistent with weak, poorly organized mantle flow beneath the region; the establishment of a coherent flow field in this region was likely inhibited by the presence of remnant slab material lodged in the uppermost mantle.

6. Summary

I have investigated the splitting of SKS phases measured at 14 stations of the NARS-Baja network surrounding the Gulf of California over the period 2002–2007 and identified 267 well-constrained splitting measurements, of which 216 were nulls. Null measurements dominated the dataset at most stations, and several stations exhibited null splitting over a wide range of backazimuths. In the northwestern part of the array, non-null measurements exhibit a great deal of variability and there is evidence for the variation of measured splitting parameters with backazimuth and over short length scales. Fast directions in this region range from NW–SE, roughly parallel to the strike of the transform plate boundary, to roughly E–W. Stations located on the Baja peninsula further to the south tend to be dominated by null measurements, which is indicative of weak and/or complex anisotropy beneath the region. Two of these stations (NE74 and NE76) exhibit average fast directions that are roughly parallel to the strike of the Gulf of California rift system. Splitting patterns at stations located to the east of the rift are variable, with one station (NE82) exhibiting a large number of well-constrained non-null measurements with no nulls identified. Average fast directions for two stations to the east of the rift are roughly parallel to the direction of absolute plate motion. The average delay time in the dataset is approximately 1.2 s, near the average value for delay times in continental regions globally. A comparison between the results obtained in this study and previous measurements provides evidence for frequency-dependent shear wave splitting, and this inference is borne out by further tests on individual SKS arrivals in the splitting dataset. The complex splitting patterns and observed frequency dependence argue for anisotropic structure that is highly heterogeneous, and both lateral and vertical variations in anisotropy are likely. This inference is consistent with measurements of 2ψ azimuthal anisotropy from previous surface wave studies in the region. One possible explanation for the complex anisotropic structure beneath the Baja Peninsula is that stalled fragments of the Magdalena and/or Guadalupe microplates, themselves remnants of the Farallon plate, have prevented a large-scale reorganization of mantle flow since the transition from convergence to oblique rifting that accompanied the cessation of Farallon subduction and the conversion of the plate boundary to largely transform motion. Anisotropy beneath stations closer to the active rifting center, particularly those located in the northern part of the Baja Peninsula, may be influenced by the small-scale centers of mantle upwelling proposed by Wang et al. (2009).

Acknowledgements

Data from the Network of Autonomously Recording Seismometers (NARS)-Baja array were used in this study and I thank the operators of the network and the Southern California Earthquake Center (SCEC) for making the data accessible to the community. Thanks to Andreas Wüstefeld and colleagues for making the SplitLab code freely available. I thank Justin Hustoft for his critical reading of the manuscript prior to submission and Raul Valenzuela for thought-provoking discussions and for his helpful comments on the paper. I am grateful to two anonymous reviewers for detailed and constructive reviews that helped to improve the manuscript considerably. This work was begun at the Department of Terrestrial Magnetism (DTM), Carnegie Institution of Washington and was supported by DTM and by Yale University.

References

Alsina, D., Snieder, R., 1995. Small-scale sublithospheric continental mantle deformation: constraints from SKS splitting observations. Geophys. J. Int. 123, 431–448.

Atwater, T.M., 1970. Implications of plate tectonics for the Cenozoic evolution of western North America. Geol. Soc. Am. Bull. 81, 3513–3536.

Bird, P., 1988. Formation of the Rocky Mountains, western United States: A continuum computer model. Science 239, 1501–1507.

Bohannon, R.G., Parsons, T., 1995. Tectonic implications of post-30 Ma Pacific and North American relative plate motions. Geol. Soc. Am. Bull. 107, 937–959.

Carter, A.J., Kendall, J.-M., 2006. Attenuation anisotropy and the relative frequency content of split shear waves. Geophys. J. Int. 165, 865–874.

Clitheroe, G., van der Hilst, R.D., 1998. Complex anisotropy in the Australian lithosphere from shear-wave splitting in broad-band SKS records. In: Braun, J., et al. (Eds.), Structure and Evolution of the Australian Continent. American Geophysical Union, pp. 73–78.

Coffin, M.F., Gahagan, L.M., Lawver, L.A., 1998, Present-day plate boundary digital data compilation. University of Texas Institute for Geophysics Technical Report no. 174.

Dixon, T., Farina, F., DeMets, C., Suarez-Vidal, F., Fletcher, J., Marquez-Azua, B., Miller, M., Sanchez, O., Umhoefer, P., 2000. New kinematic models for Pacific–North America motion from 3 Ma to present, II. Evidence for a "Baja California shear zone. Geophys. Res. Lett. 27, 3961–3964.

Favier, N., Chevrot, S., 2003. Sensitivity kernels for shear wave splitting in transverse isotropic media. Geophys. J. Int. 167, 1332–1352.

Favier, N., Chevrot, S., Komatitsch, D., 2004. Near-field influences on shear wave splitting and traveltime sensitivity kernels. Geophys. J. Int. 156, 467–482.

Fouch, M.J., Fischer, K.M., 1998. Shear wave anisotropy in the Mariana subduction zone. Geophys. Res. Lett. 25, 1221–1224.

Gao, S., Davis, P.M., Liu, H., Slack, P.D., Rigor, A.W., Zorin, Y.A., Mordvinova, V.V., Kozhevnikov, V.M., Logatchev, N.A., 1997. SKS splitting beneath continental rift zones. J. Geophys. Res. 102, 22781–22797.

González, M., Munguía, L., 2003. Seismic anisotropy observations in the Mexicali Valley, Baja California, Mexico. Pure Appl. Geophys. 160, 2257–2278.

Greve, S.M., Savage, M.K., Hofmann, S.D., 2008. Strong variations in seismic anisotropy across the Hikurangi subduction zone, North Island, New Zealand. Tectonophysics 462, 7–21.

Gripp, A.E., Gordon, R.G., 2002. Young tracks of hot spots and current plate velocities. Geophys. J. Int. 150, 321–361.

Hartog, R., Schwartz, S.Y., 2001. Depth-dependent mantle anisotropy below the San Andreas fault system: apparent splitting parameters and waveforms. J. Geophys. Res. 106, 4155–4167.

Henry, C.D., 1989. Late Cenozoic Basin and Range structure in western Mexico adjacent to the Gulf of California. Geol. Soc. Am. Bull. 101, 1147–1156.

Holtzman, B.K., Kohlstedt, D.L., Zimmerman, M.E., Heidelbach, F., Hiraga, T., Hustoft, J., 2003. Melt segregation and strain partitioning: implications for seismic anisotropy and mantle flow. Science 301, 1227–1230.

Jung, H., Mo, W., Green, H.W., 2009. Upper mantle seismic anisotropy resulting from pressure-induced slip transition in olivine. Nat. Geosci. 2, 73–77.

Kaminski, É., Ribe, N.M., 2002. Timescales for the evolution of seismic anisotropy in mantle flow. Geochem. Geophys. Geosyst. 3 (8), 1051, doi:10.1029/2001GC000222.

Karato, S., Jung, H., Katayama, I., Skemer, P., 2008. Geodynamic significance of seismic anisotropy of the upper mantle: new insights from laboratory studies. Annu. Rev. Earth Planet. Sci 36, 59–95.

Lebedev, S., van der Hilst, R.D., 2008. Global upper-mantle tomography with the automated multimode inversion of surface and S-wave forms. Geophys. J. Int. 162, 951–964.

Lewis, J.L., Day, S.M., Magistrale, H., Castro, R.R., Astiz, L., Rebollar, C., Eakins, J., Vernon, F.L., Brune, J.N., 2001. Crustal thickness of the Peninsular Ranges and Gulf Extensional Province in the Californias. J. Geophys. Res. 106, 13599–13611.

Liu, E., Maultzsch, S., Chapman, M., Li, X.Y., Queen, J.H., Zhang, Z., 2003. Frequency-dependent seismic anisotropy and its implications for estimating fracture size in low porosity reservoirs. The Leading Edge 22, 662–665.

Lizzaralde, D., Axen, G.J., Brown, H.E., Fletcher, J.M., González-Fernández, A., Harding, A.J., Holbrook, W.S., Kent, G.M., Paramo, P., Sutherland, F., Umhoefer, P.J., 2007. Variation in styles of rifting in the Gulf of California. Nature 448, 466–469.

Long, M.D., 2009. Complex anisotropy in D" beneath the eastern Pacific from SKS–SKKS splitting discrepancies. Earth Planet. Sci. Lett. 283, 181–189.

Long, M.D., de Hoop, M.V., van der Hilst, R.D., 2008. Wave-equation shear wave splitting tomography. Geophys. J. Int. 172, 311–330.

Long, M.D., Gao, H., Klaus, A., Wagner, L.S., Fouch, M.J., James, D.E., Humphreys, E.D., 2009. Shear wave splitting and the pattern of mantle flow beneath eastern Oregon. Earth Planet. Sci. Lett. 288, 359–369.

Long, M.D., Silver, P.G., 2009. Shear wave splitting and mantle anisotropy: measurements, interpretations, and new directions. Surv. Geophys. 30, 407–461.

Long, M.D., van der Hilst, R.D., 2005a. Estimating shear wave splitting parameters from broadband recordings in Japan: a comparison of three methods. Bull. Seism. Soc. Am. 95, 1346–1358.

Long, M.D., van der Hilst, R.D., 2005b. Upper mantle anisotropy beneath Japan from shear wave splitting. Phys. Earth Planet. Inter. 151, 206–222.

Marson-Pidgeon, K., Savage, M.K., 1997. Frequency-dependent anisotropy in Wellington, New Zealand. Geophys. Res. Lett. 24, 3297–3300.

Meade, C., Silver, P.G., Kaneshima, S., 1995. Laboratory and seismological observations of lower mantle isotropy. Geophys. Res. Lett. 22, 1293–1296.

Michaud, F., Royer, J.Y., Bourgois, J., Dyment, J., Calmus, T., Bandy, W., Sosson, M., Mortera-Gutiérrez, C., Sichler, B., Rebolledo-Viera, M., Pontoise, B., 2006. Oceanic-ridge subduction vs. slab break off: plate tectonic evolution along the Baja California Sur continental margin since 15 Ma. Geology 34, 13–16.

Nettles, M., Dziewonski, A.M., 2008. Radially anisotropic shear velocity structure of the upper mantle globally and beneath North America. J. Geophys. Res. 113, B02303, doi:10.1029/2006JB004819.

Niu, F., Perez, A.M., 2004. Seismic anisotropy in the lower mantle: a comparison of waveform splitting of SKS and SKKS. Geophys. Res. Lett. 31, L24612, doi:10.1029/2004GL0211196.

Obrebski, M., Castro, R.R., 2008. Seismic anisotropy in northern and central Gulf of California region, Mexico, from receiver functions and new evidence of possible plate capture. J. Geophys. Res. 113, B03301, doi:10.1029/2007JB005156.

Obrebski, M., Castro, R.R., Valenzuela, R.W., van Benthem, S., Rebollar, C.J., 2006. Shear-wave splitting observations at the regions of northern Baja California and southern Basin and Range in Mexico. Geophys. Res. Lett. 33, L05302, doi:10.1029/2005GL024720.

Oskin, M., Stock, J.M., Martín-Barajas, 2001. Rapid localization of Pacific–North America plate motion in the Gulf of California. Geology 29, 459–463.

Persaud, P., Pérez-Campos, X., Clayton, R.W., 2007. Crustal thickness variations in the margins of the Gulf of California from receiver functions. Geophys. J. Int. 170, 687–699.

Polet, J., Kanamori, H., 2002. Anisotropy beneath California: Shear wave spitting measurements using a dense broadband array. Geophys. J. Int. 149, 313–327.

Pozgay, S.H., Wiens, D.A., Conder, J.A., Shiobara, H., Sugioka, H., 2007. Complex mantle flow in the Mariana subduction system: evidence from shear wave splitting. Geophys. J. Int. 170, 371–386.

Rümpker, G., Tommasi, A., Kendall, J.-M., 1999. Numerical simulations of depth-dependent anisotropy and frequency-dependent wave propagation effects. J. Geophys. Res. 104, 23141–23153.

Saltzer, R.L., Gaherty, J., Jordan, T.H., 2000. How are vertical shear wave splitting measurement affected by variations in the orientation of azimuthal anisotropy with depth? Geophys. J. Int. 141, 374–390.

Sedlock, R.L., 2003. Geology and tectonics of the Baja California peninsula and adjacent areas. Geol. Soc. Am. Spec. Pap. 374, 1–42.

Silver, P.G., 1996. Seismic anisotropy beneath the continents: probing the depths of geology. Annu. Rev. Earth Planet. Sci. 24, 385–432.

Silver, P.G., Chan, W.W., 1991. Shear wave splitting and subcontinental mantle deformation. J. Geophys. Res. 96, 16429–16454.

Stock, J.M., Hodges, K.V., 1989. Pre-Pliocene extension around the Gulf of California and the transfer of Baja California to the Pacific Plate. Tectonics 8, 99–115.

Suter, M., Contreras, J., 2002. Active tectonics of northeastern Sonora, Mexico (southern Basin and Range Province) and the 3 May 1887 M_w 7.4 earthquake. Bull. Seism. Soc. Am. 92, 581–589.

Trampert, J., Paulssen, H., van Wettum, A., Ritsema, J., Clayton, R., Castro, R.R., Rebollar, C.J., Pérez-Verti, A., 2003. New array monitors seismic activity near the Gulf of California in Mexico. Eos Trans. AGU 84, 29–32.

van Benthem, S.A.C., Valenzuela, R.W., Obrebski, M., Castro, R.R., 2008. Measurements of upper mantle shear wave anisotropy from stations around the southern Gulf of California. Geofis. Int. 47, 127–144.

Vauchez, A., Tommasi, A., Barruol, G., Maumus, J., 2000. Upper mantle deformation and seismic anisotropy in continental rifts. Phys. Chem. Earth (A) 25, 111–117.

Vecsey, L., Plomerová, J., Babuska, V., 2008. Shear wave splitting measurements: problems and solutions. Tectonophysics 462, 178–196.

Wang, Y., Forsyth, D.W., Savage, B., 2009. Convective upwelling in the mantle beneath the Gulf of California. Nature 462, 499–502.

Wirth, E., Long, M.D., 2010. Frequency-dependent shear wave splitting beneath the Japan and Izu-Bonin subduction zones. Phys. Earth Planet. Inter., in press, doi:10.1016/j.pepi.05.006.

Wüstefeld, A., Bokelmann, G., 2007. Null detection in shear-wave splitting measurements. Bull. Seism. Soc. Am. 97, 1204–1211.

Wüstefeld, A., Bokelmann, G., Barruol, G., Zaroli, C., 2007. Splitlab: a shear-wave splitting environment in Matlab. Comp. Geosci. 34, 515–528.

Zhang, X., Paulssen, H., Lebedev, S., Meier, T., 2007. Surface wave tomography of the Gulf of California. Geophys. Res. Lett. 34, L15305, doi:10.1029/2007GL030631.

Zhang, X., Paulssen, H., Lebedev, S., Meier, T., 2009. 3D shear velocity structure beneath the Gulf of California from Rayleigh wave dispersion. Earth Planet. Sci. Lett. 279, 255–262.

Zúñiga, F.R., Castro, R.R., Domínguez, T., 1995. Stress orientation and anisotropy based on shear-wave splitting observations in the Cerro Prieto fault area, Baja California, Mexico. Pure Appl. Geophys. 144, 39–57.